Journal of Alloys and Compounds 820 (2020) 153078

Contents lists available at ScienceDirect

Journal of Alloys and Compounds

journal homepage: http://www.elsevier.com/locate/jalcom

Influence of thermo-mechanical processing on structure and mechanical properties of a new metastable β Ti−29Nb−2Mo−6Zr alloy with low Young's modulus

Aline Raquel Vieira Nunes [a, *], Sinara Borborema [b], Leonardo Sales Araújo [a], Loïc Malet [c], Jean Dille [c], Luiz Henrique de Almeida [a]

[a] Universidade Federal do Rio de Janeiro, Rio de Janeiro, RJ, 21.941-972, Brazil
[b] Faculdade de Tecnologia Campus Regional de Resende – FAT/UERJ, Resende, RJ, Brazil
[c] Université Libre de Bruxelles, Brussels, Belgium

ARTICLE INFO

Article history:
Received 30 September 2018
Received in revised form
28 October 2019
Accepted 17 November 2019
Available online 19 November 2019

Keywords:
Titanium alloys
Microstructure
Cold rolling
Texture evolution
Orthopedic applications

ABSTRACT

A low Young's modulus is required for titanium alloys used in orthopedic implants, such as hip prosthetic stems, in order to avoid stress shielding due to a large difference in Young's modulus between the prosthetic stem and the cortical bone. The low Young's modulus has been observed to occur in metastable β-Ti alloys by precipitation of a stress-induced α″ martensite during cold deformation. Under this context, the Influence of thermo-mechanical processing on the microstructure and mechanical properties of the metastable β Ti−29Nb−2Mo−6Zr alloy was studied as well as the influence of the degree of deformation by cold rolling with subsequent annealing after homogenization heat treatment. The alloy presents a β microstructure after solution heat treatment at 1000 °C for 24h, followed by water quenching, while posterior cold rolling induces the precipitation of α" martensite. Young's modulus decreases and hardness increases with the degree of deformation. The annealed samples showed higher hardness and Young's modulus than the cold rolled samples. A thickness reduction of 90% maximizes the hardness/Young's modulus ratio and optimizes the required mechanical properties for orthopedic implants. The results indicate that the alloy is a promising alternative for the widely used Ti−6Al−4V.

1. Introduction

Titanium (Ti) and its alloys are widely used as orthopedic implants due to good corrosion and fatigue resistance, biocompatibility, good mechanical properties and lower modulus of elasticity than other metallic biomaterials such as stainless steel and Co−Cr-based alloys. Young's modulus is one most important factors in the selection of a material for biomedical purposes in orthopedic implants, owing to the fact that low values will allow a better distribution of stresses as its value is closer to the Young's modulus of the bone [1–9].

In general, the most used Ti alloy in orthopedic applications is the Ti−6Al−4V (α + β class). Although this alloy has a lower Young's modulus when compared to other materials, however it is still high compared to that of bone tissue [6]. Studies of this alloy have also shown that the release of small amounts of V and Al in the human body may induce cytotoxic effects and neurological disorders, which has led over the last decade to the development of new Ti alloys [9].

Among titanium alloys the most appropriate for orthopedic implants are those of β-type [4,8,10–13]. The superiority of these alloys is more pronounced in the solution treated and aged conditions, in which the β grain size, volume fraction, morphology, size and free mean path of precipitates control the resistance levels [11,14,15]. These alloys are basically composed by titanium plus betagenic, non-toxic and biocompatible elements, such as Mo, Nb, Ta, Sn and Zr. Neacsu studied the in vitro biocompatibility of new β-Ti alloys Ti−12Mo, Ti−4Mo−32Nb, Ti−6Mo−24Nb, Ti−8Mo−16Nb and Ti−10Mo−8Nb evidencing its very good biocompatibility [16]. The β phase exhibits a lower Young's modulus than α and α + β phases, and the β alloys satisfy most of the requirements of an ideal material for biomedical implants [5,10,12].

A low Young's modulus is required for titanium alloys used in orthopedic implants, such as hip prosthetic stems, in order to avoid

* Corresponding author.
E-mail address: alineraquel@metalmat.ufrj.br (A.R. Vieira Nunes).

https://doi.org/10.1016/j.jallcom.2019.153078
0925-8388/

Table 1
Chemical composition and [wt%Mo]eq for Ti−29Nb−2Mo−6Zr alloy.

Alloy (% mass)	Ti	Mo	Nb	Zr	$[Mo_{eq}]$%
Ti−29Nb−2Mo−6Zr	76.75	1.22	18.20	3.84	10.12

stress shielding induced by a large difference in Young's modulus between the prosthetic stem and the cortical bone. The low Young's modulus has been observed to occur in metastable β-Ti alloys by precipitation stress-induced α″ martensite during cold rolling through the preferred texture development. It has been reported that rolled/swaged Ti-33.6Nb−4Sn alloy presented a 40 GPa young's modulus due to <010>-textured α″ martensite and <110>-textured β phases along the rolling direction [17]. Besides this mechanism, there are others mechanisms related to cold deformation as dislocations slip and deformation twins. It has been shown that α" phase precipitation and two specific twinning modes, {112}<111> type and {332}<113> type, could be activated under different stress conditions in some β-type Ti alloys [18−20].

Several promising metastable β-type Ti alloys have been developed for orthopedic implants such as Ti−Zr−Nb−Ta, Ti−Nb−Zr, Ti−Sn−Nb−Ta, Ti−Sn−Nb−Ta, Ti-Mo-Nb and

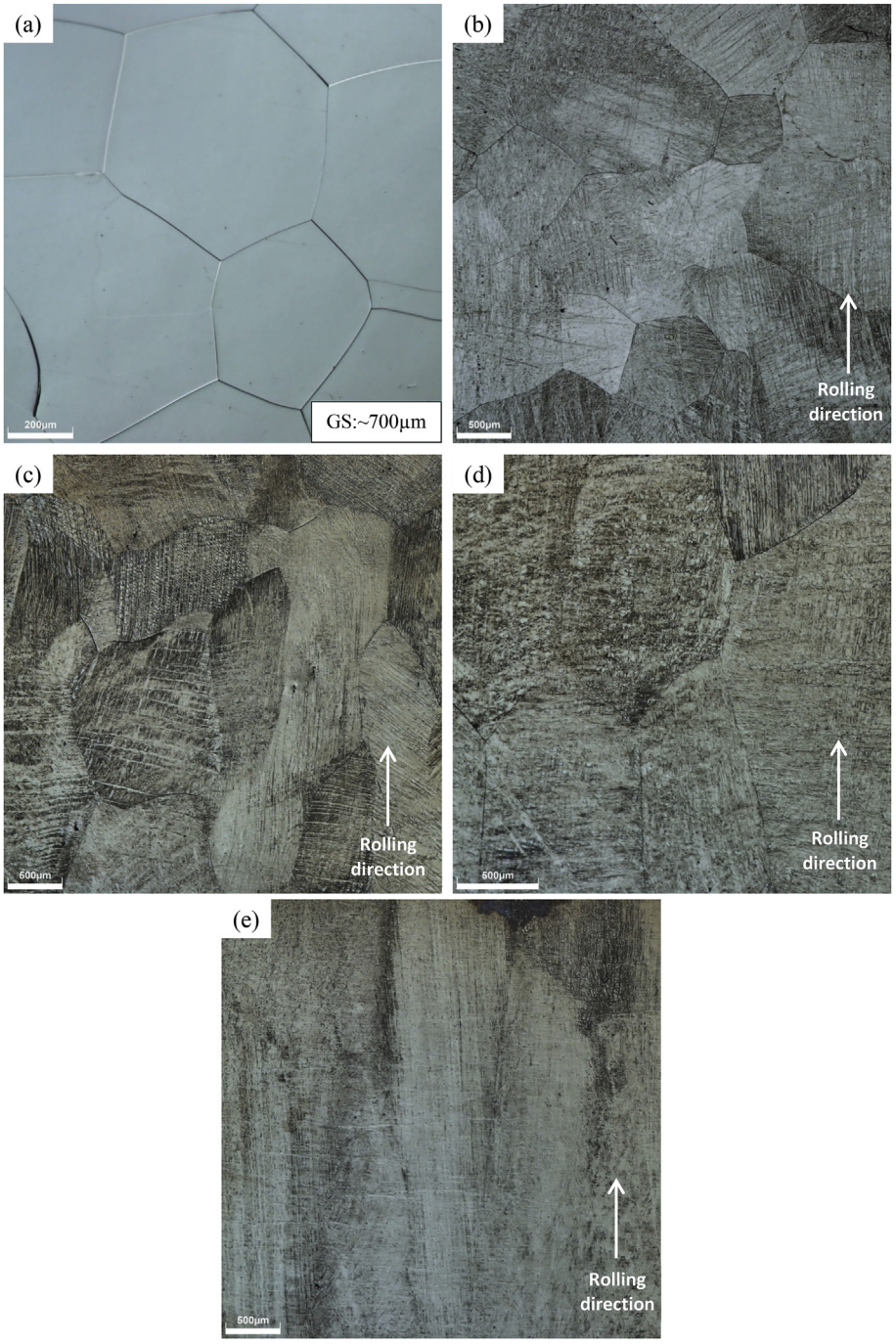

Fig. 1. OM microstructures of the Ti−29Nb−2Mo−6Zr alloy: (a) homogenized at 1000 °C/24 h and water quenched and with (b) subsequently cold rolled with 30%, (c) 50%, (d) 70% and (e) 90% thickness reduction.

Ti–Nb–Ta–Mo [2–5,17–19] and, for these alloys, Young's modulus varies between 50 and 95 GPa due to the alloy composition, thermomechanical treatments and a bi-phased (α"+β) microstructure [3,10,12]. Studies show that it is not trivial to obtain low Young's modulus and high strength simultaneously in Ti alloys [14]. The chemical composition of the new metastable Ti-β metastable Ti–29Nb–2Mo–6Zr alloy was previously studied [21]. The choice of the chemical composition was determined from the phase stability diagram proposed by Abdel-Hady and based on $\overline{Bo}$ and $\overline{Md}$ parameters, where, $\overline{Bo}$ is the average bond order between atoms and $\overline{Md}$ is the average d-orbital energy level of the element in the alloy [22].

This study analyzes the influence of cold deformation on the microstructure, texture evolution and mechanical properties of the Ti-β metastable Ti–29Nb–2Mo–6Zr alloy. Therefore, a single-phase β structure after homogenization heat, followed by water quenching was obtained. The α" martensite was induced during cold rolling. Subsequent annealing recovers the single-phase β structure, this time with improved behavior. The objective of this work is to study the alloy's microstructure and to verify if it can be considered as an interesting substitute to the Ti–6Al–4V alloy currently used for orthopedic applications.

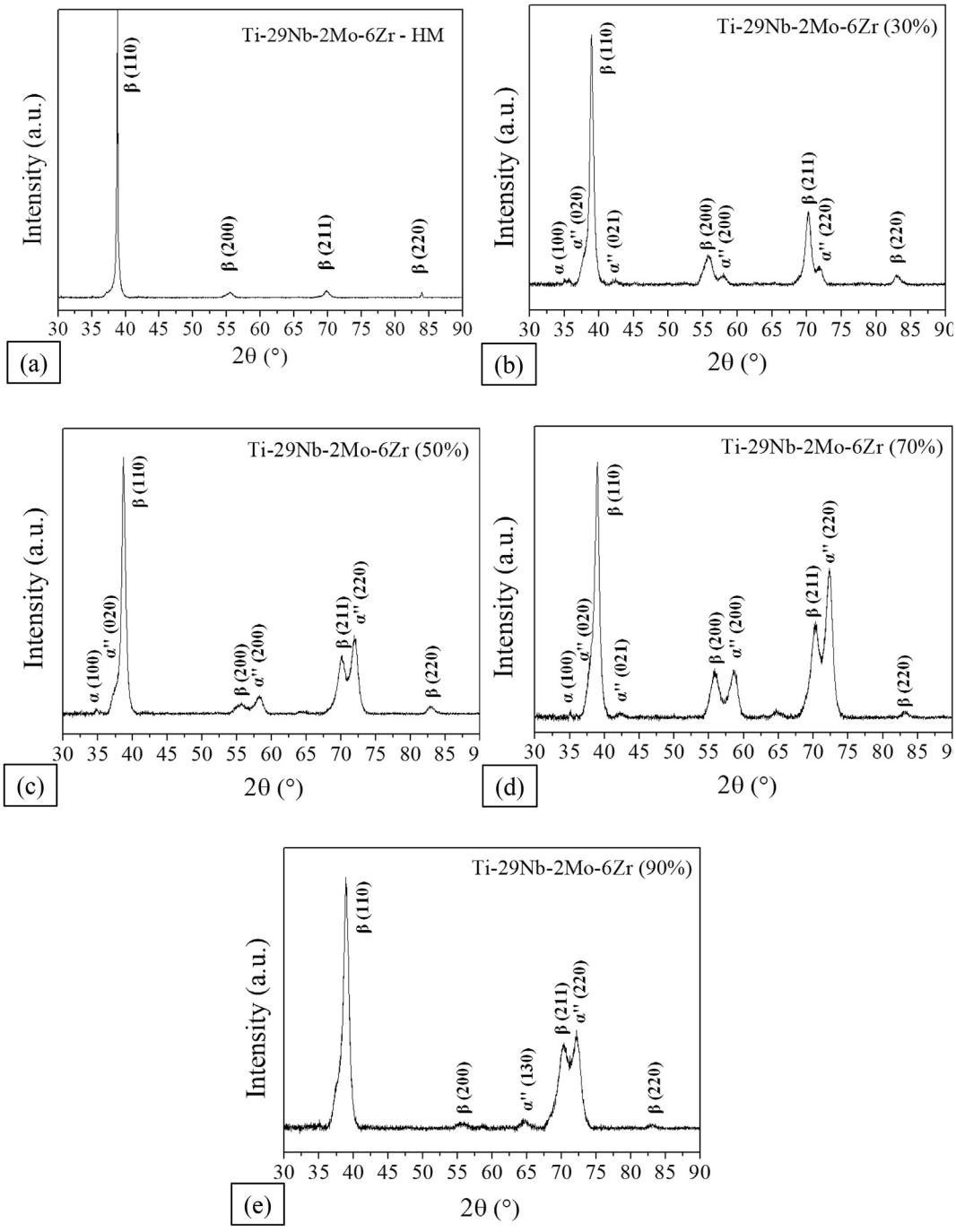

Fig. 2. X-ray diffraction patterns of: (a) homogenized at 1000 °C/24 h and water quenched: (b) 30%, (c) 50%, (d) 70% and (e) 90% cold rolled of Ti–29Nb–2Mo–6Zr alloy measured through the rolling plane.

2. Material and methods

An ingot of the Ti–29Nb–2Mo–6Zr alloy was produced from commercially pure Ti (ASTM F67), Mo (>99.9%, Plansee Group, Austria), Nb (>99.9%, EEL/USP, Brazil) and Zr (Nuclear grade) by arc melting process with a tungsten electrode and a water-cooled copper hearth. This ingot was prepared under a high purity argon atmosphere (>99.9999% pure) and was then re-melted eight times to improve the chemical homogeneity. The obtained ingot (60g - 17x12 × 70 mm) was homogenized (HM) at 1000 °C under argon atmosphere for 24 h and then quenched in water at room temperature. Subsequently, the ingot was cold rolled (CR) with reductions of 30%, 50%, 70% and 90%, followed by annealing at 950 °C for 1h and quenched in water at room temperature.

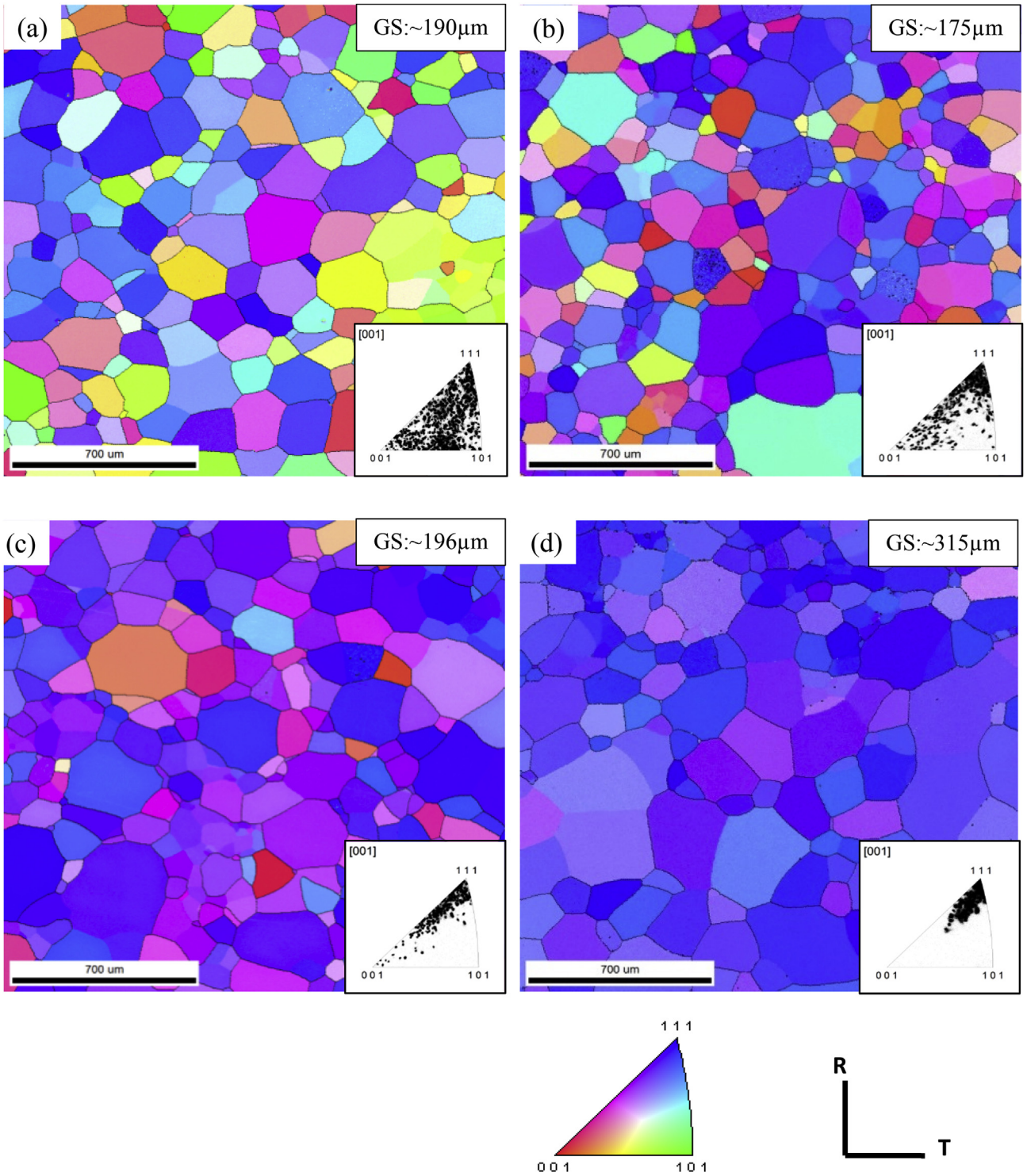

Fig. 3. Inverse pole figure maps created by EBSD-OIM of cold rolled Ti–29Nb–2Mo–6Zr alloy, followed by annealing at 950 °C for 1h, showing texture evolution with the inverse pole figure (IPF) analyzed on the rolling plane of samples. (a) 30%, (b) 50%, (c) 70% and (d) 90% cold rolled/annealed.

Phase identification was carried out by X-ray Diffraction (XRD), Shimadzu model XRD 6000 diffractometer, operated at 40 kV and 30 mA, using a Ni-filtered CuK$_\alpha$ radiation. Structural characterization was performed by Optical Microscopy (OM) and Electron Backscattered Diffraction (EBSD) analysis. For OM and EBSD characterization, the samples were ground with sandpaper from 100 to 2400 mesh and polished with 90% colloidal silica and 10% distilled water solution for 30 min and then etched with Kroll's reagent (8 mL HF, 20 mL HNO_3 and 62 mL H_2O). EBSD measurements were performed on a Hitachi SU70 FEG-SEM operated at 20 kV and equipped with an EDAX HIKARI camera. A step size of 3 μm was used. Orientation mapping analyses were done using the TSL OIM software. Vickers microhardness H_V values were measured using a DHV-1000 Micro Vickers Hardness Tester with a 200 gf load for 15 s. The values presented represent the average of ten measurements. The Young's modulus (YM) was determined by indentation technique using an Agilent G200 nanoindenter with 6 sets of 6 indentations made using a Berkovich tip with a maximum applied load of 100 mN. The obtained modulus was the average of 36 measurements.

3. Results and discussion

3.1. Microstructural characterization

The chemical composition of the alloy is shown in Table 1, as well as the calculated [wt%Mo]eq for the alloy. Molybdenum equivalence ([wt%Mo]eq) of 10% or higher is required to stabilize the β phase upon water quenching [15]. Therefore, this alloy satisfies the required condition to obtain a single-phase β microstructure after homogenization heat treatment and water quenching.

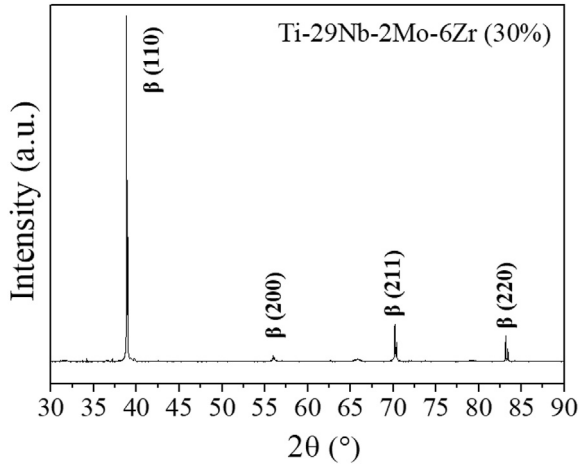

Fig. 4. X-ray diffraction pattern of 30% cold rolled Ti−29Nb−2Mo−6Zr alloy followed by annealing at 950 °C for 1h.

Fig. 1 shows by OM the microstructural evolution after cold rolling of the Ti−29Nb−2Mo−6Zr alloy with cold reductions of 30%, 50%, 70% and 90%. It was found that the microstructure of the HM sample presents single-phase equiaxial β grains with the size in the range of 500−700 μm after solution heat treatment at 1000 °C for 24h followed by water quenching (Fig. 1(a)). After 30% cold rolling the microstructure shows grains with visible deformation bands (Fig. 1 (b)). After 50% CR sample shows that the grains are elongated, and the deformation bands are visible within the deformed grains (Fig. 1 (c)). As the reduction increases, the deformation bands are gradually distorted, as seen in Fig. 1(d), after 70% CR. And after 90% CR, the sample exhibits a microstructure with fibrous stripes, owing to the severe cold deformation. Precipitation of the α" phase could not be observed in the β matrix due to the inherently small size.

Fig. 2 presents the XRD patterns of the Ti−29Nb−2Mo−6Zr alloy HM and CR with the cold reductions of 30%, 50%, 70% and 90%. For homogenized Ti−29Nb−2Mo−6Zr alloy, the XRD pattern reveals only peaks corresponding to β phase. After cold rolling, the diffraction patterns show orthorhombic α" phase peaks that were seen in all samples, indicating that stress-induced martensitic phase (β to α" transformation) occurred during cold rolling. The intensity of α" martensite peaks increased gradually with increasing rolling reduction until 70% CR. On the other hand, the intensity of α" peaks decreased after 90% of cold rolling reduction, as shown in Fig. 2(e), what can be attributed to the intense texture of the β phase.

The EBSD inverse pole figure (IPF) maps in Fig. 3 show the texture evolution of Ti−29Nb−2Mo−6Zr alloy annealed for 1h at 950 °C after cold rolling in function of the reduction rate. The first information indicated in Fig. 3 is that the annealed samples are all constituted of equiaxed β grains. This is confirmed by the XRD pattern in Fig. 4. This XRD pattern reveals only peaks corresponding to the β phase. On the other hand, the comparison of the different IPF maps indicates a progressive formation of a ⟨111⟩β texture when the reduction rate increases. After 90% cold rolling and annealing, the sample exhibits a strong ⟨111⟩β texture.

3.2. Hardness/young's modulus ratio

Table 2 shows the Vickers hardness, Young's modulus and the hardness to Young's modulus ratio of the Ti−29Nb−2Mo−6Zr alloy for the homogenized, cold rolled and annealed and water quenching after cold rolled. Data for Ti−6Al−4V alloy were also included in Table 2 as a reference. The microhardness measurements increased with the degree of deformation.

Table 2 shows the Young's modulus measured using the instrumented indentation technique. Comparing the value of the 90% cold rolled alloy with reference Ti−6Al−4V alloy, a 54% reduction was evidenced (from 140 GPa to 76 GPa). As a consequence, a higher HV/YM ratio (3.65) was obtained for the experimental alloy. The sample with 90% cold rolled, annealed and water quenched also showed a high value for the HV/YM ratio (3.72). This

Table 2
Vickers microhardness (HV), Young's Modulus (YM) and HV/YM ratio of Ti−29Nb−2Mo−6Zr alloy cold rolled and annealed and water quenching after cold rolling.

Reduct.	Homogenized and Cold Rolled			Annealed and Water Quenching after Cold Rolling		
	Microhardness (HV)	YM (GPa)	HV to YM ratio	Microhardness (HV)	YM (GPa)	HV to YM ratio
Homogenized	228.39 ± 5.58	92.55 ± 3.13	2.47		–	–
Cold rolled −30%	230.92 ± 4.83	83.46 ± 3.39	2.77	259.63 ± 2.73	89.77 ± 1.66	2.90
Cold rolled −50%	239.98 ± 5.32	84.97 ± 2.85	2.82	269.58 ± 4.55	90.85 ± 0.86	2.92
Cold rolled −70%	243.37 ± 3.85	83.01 ± 3.32	2.93	274.57 ± 2.94	87.64 ± 2.15	3.12
Cold rolled −90%	278.37 ± 3.71	76.36 ± 2.25	3.65	296.66 ± 3.22	79.32 ± 0.55	3.72
Ti−6Al−4V [23]	337 ± 16.0	140 ± 3.70	2.40	–	–	–

can be explained by the transformation of α" into β after annealing and quenching, as well as due to the formation of a strong crystallographic texture. The Young's modulus values are also directly associated with the volume fraction of β and α" in these alloys [2].

4. Conclusions

The new Ti−29Nb−2Mo−6Zr alloy presents a single-phase β microstructure after solution heat treatment at 1000 °C for 24h followed by water quenching. Subsequent cold rolling induces the precipitation of α" martensite in the β phase, with back transformation to β phase after annealing treatment. As a general observation, Young's modulus decreased whereas the hardness increases with increasing degree of deformation. The sample cold rolled to 90% exhibits the lowest Young's modulus, however, after annealing exhibits the highest HV/YM ratio. All conditions presented a higher HV/YM ratio when compared to Ti−6Al−4V alloy. The Ti−29Nb−2Mo−6Zr alloy is a promising substitute to the conventional Ti−6Al−4V alloy for biomedical applications.

Acknowledgements

This study was financed in part by the Coordenação de Aperfeiçoamento de Pessoal de Nível Superior - Brasil (CAPES) - Finance Code 001, CNPq and FAPERJ.

References

[1] J. Tiley, T. Searles, E. Lee, S. Kar, R. Banerjee, J.C. Russ, H.L. Fraser, Quantification of microstructural features in α/β titanium alloys, Mater. Sci. Eng. A 372 (2004) 191−198, https://doi.org/10.1016/j.msea.2003.12.008.
[2] S.B. Gabriel, C.A. Nunes, G.D.A. Soares, Production, microstructural characterization and mechanical properties of As-Cast Ti-10Mo-xNb alloys, Artif. Organs 32 (2008) 299−304, https://doi.org/10.1111/j.1525-1594.2008.00546.x.
[3] D.M. Gordin, T. Gloriant, G. Nemtoi, R. Chelariu, N. Aelenei, A. Guillou, D. Ansel, Synthesis, structure and electrochemical behavior of a beta Ti-12Mo-5Ta alloy as new biomaterial, Mater. Lett. 59 (2005) 2959−2964, https://doi.org/10.1016/j.matlet.2004.09.064.
[4] D. Kuroda, M. Niinomi, M. Morinaga, Y. Kato, T. Yashiro, Design and mechanical properties of new β type titanium alloys for implant materials, Mater. Sci. Eng. A 243 (1998) 244−249, https://doi.org/10.1016/S0921-5093(97)00808-3.
[5] S.J. Li, R. Yang, S. Li, Y.L. Hao, Y.Y. Cui, M. Niinomi, Z.X. Guo, Wear characteristics of Ti-Nb-Ta-Zr and Ti-6Al-4V alloys for biomedical applications, Wear 257 (2004) 869−876, https://doi.org/10.1016/j.wear.2004.04.001.
[6] P. Majumdar, S.B. Singh, M. Chakraborty, Elastic modulus of biomedical titanium alloys by nano-indentation and ultrasonic techniques-A comparative study, Mater. Sci. Eng. A 489 (2008) 419−425, https://doi.org/10.1016/j.msea.2007.12.029.
[7] S. Nag, R. Banerjee, H.L. Fraser, A novel combinatorial approach for understanding microstructural evolution and its relationship to mechanical properties in metallic biomaterials, Acta Biomater. 3 (2007) 369−376, https://doi.org/10.1016/j.actbio.2006.08.005.
[8] M. Niinomi, T. Akahori, T. Takeuchi, S. Katsura, H. Fukui, H. Toda, Mechanical properties and cyto-toxicity of new beta type titanium alloy with low melting points for dental applications, Mater. Sci. Eng. C 25 (2005) 417−425, https://doi.org/10.1016/j.msec.2005.01.024.
[9] D. Raabe, B. Sander, M. Friák, D. Ma, J. Neugebauer, Theory-guided bottom-up design of β-titanium alloys as biomaterials based on first principles calculations: theory and experiments, Acta Mater. 55 (2007) 4475−4487, https://doi.org/10.1016/j.actamat.2007.04.024.
[10] M. Abdel-Hady Gepreel, M. Niinomi, Biocompatibility of Ti-alloys for long-term implantation, J. Mech. Behav. Biomed. Mater. 20 (2013), https://doi.org/10.1016/j.jmbbm.2012.11.014.
[11] M. Niinomi, M. Nakai, J. Hieda, Development of new metallic alloys for biomedical applications, Acta Biomater. 8 (2012) 3888−3903, https://doi.org/10.1016/j.actbio.2012.06.037.
[12] M. Long, H.J. Rack, Titanium alloys in total joint replacement–a materials science perspective, Biomaterials 19 (1998) 1621−1639, https://doi.org/10.1016/S0142-9612(97)00146-4.
[13] M. Niinomi, Biologically and mechanically biocompatible titanium alloys, Mater. Trans. 49 (2008) 2170−2178, https://doi.org/10.2320/matertrans.L-MRA2008828.
[14] H. Matsumoto, S. Watanabe, S. Hanada, Microstructures and mechanical properties of metastable β TiNbSn alloys cold rolled and heat treated, J. Alloy. Comp. 439 (2007) 146−155, https://doi.org/10.1016/j.jallcom.2006.08.267.
[15] O.M. Ivasishin, P.E. Markovsky, Y.V. Matviychuk, S.L. Semiatin, C.H. Ward, S. Fox, A comparative study of the mechanical properties of high-strength β-titanium alloys, J. Alloy. Comp. 457 (2008) 296−309, https://doi.org/10.1016/j.jallcom.2007.03.070.
[16] P. Neacsu, D.M. Gordin, V. Mitran, T. Gloriant, M. Costache, A. Cimpean, In vitro performance assessment of new beta Ti-Mo-Nb alloy compositions, Mater. Sci. Eng. C 47 (2015) 105−113, https://doi.org/10.1016/j.msec.2014.11.023.
[17] T.K. Jung, H.S. Lee, S. Semboshi, N. Masahashi, T. Abumiya, S. Hanada, A new concept of hip joint stem and its fabrication using metastable TiNbSn alloy, J. Alloy. Comp. 536 (2012) S582−S585, https://doi.org/10.1016/j.jallcom.2011.12.077.
[18] F. Sun, J.Y. Zhang, M. Marteleur, T. Gloriant, P. Vermaut, D. Laillé, P. Castany, C. Curfs, P.J. Jacques, F. Prima, Investigation of early stage deformation mechanisms in a metastable β titanium alloy showing combined twinning-induced plasticity and transformation-induced plasticity effects, Acta Mater. 61 (2013) 6406−6417, https://doi.org/10.1016/j.actamat.2013.07.019.
[19] M. Ahmed, A.A. Gazder, A.A. Saleh, D. Wexler, E.V. Pereloma, Stress-induced twinning and phase transformations during the compression of a Ti-10V-3Fe-3Al alloy, Metall. Mater. Trans. A Phys. Metall. Mater. Sci. 48 (2017) 2791−2800, https://doi.org/10.1007/s11661-016-3675-4.
[20] L. Wang, W. Lu, J. Qin, F. Zhang, D. Zhang, Microstructure and mechanical properties of cold-rolled TiNbTaZr biomedical β titanium alloy, Mater. Sci. Eng. A 490 (2008) 421−426, https://doi.org/10.1016/j.msea.2008.03.003.
[21] A.R.V. Nunes, S. Borborema, L.S. Araújo, J. Dille, L. Malet, L.H. de Almeida, Production, microstructure and mechanical properties of cold-rolled Ti-Nb-Mo-Zr alloys for orthopedic applications, J. Alloy. Comp. 743 (2018) 141−145, https://doi.org/10.1016/j.jallcom.2018.01.305.
[22] M. Abdel-Hady, K. Hinoshita, M. Morinaga, General approach to phase stability and elastic properties of β-type Ti-alloys using electronic parameters, Scr. Mater. 55 (2006) 477−480, https://doi.org/10.1016/j.scriptamat.2006.04.022.
[23] S. Anken, C.A. Greene, Recent developments in microstructure/property relationships of beta titanium alloys, Mater. Sci. Eng. A 263 (1999) 127−131.